

Relative Rigidity of Cell–Substrate Effects on Hepatic and Hepatocellular Carcinoma Cell Migration

Yanzi Yangben , Hongbing Wang , Li Zhong , Martin Y.M. Chiang , Qiaoyan Tan , Gurinder K. Singh , Song Li & Li Yang

To cite this article: Yanzi Yangben , Hongbing Wang , Li Zhong , Martin Y.M. Chiang , Qiaoyan Tan , Gurinder K. Singh , Song Li & Li Yang (2013) Relative Rigidity of Cell–Substrate Effects on Hepatic and Hepatocellular Carcinoma Cell Migration, Journal of Biomaterials Science, Polymer Edition, 24:2, 148-157

To link to this article: <http://dx.doi.org/10.1163/156856212X627856>



Published online: 11 May 2012.



Submit your article to this journal [↗](#)



Article views: 62



View related articles [↗](#)

Relative Rigidity of Cell–Substrate Effects on Hepatic and Hepatocellular Carcinoma Cell Migration

Yanzi Yangben^{a,b}, Hongbing Wang^{a,b}, Li Zhong^{a,b}, Martin Y. M. Chiang^c,
Qiaoyan Tan^{a,b}, Gurinder K. Singh^{a,b}, Song Li^d and Li Yang^{a,b,*}

^a Key Laboratory of Biorheological Science and Technology (Chongqing University), Ministry of Education, Bioengineering College, Chongqing University, Chongqing 400044, P. R. China

^b ‘111’ Project Laboratory of Biomechanics and Tissue Repair, Bioengineering College, Chongqing University, Chongqing 400044, P. R. China

^c Polymers Division, National Institute of Standards and Technology, Gaithersburg, MD 20899, USA

^d Department of Bioengineering, University of California, Berkeley, CA 94720, USA

Received 8 July 2011; accepted 24 January 2012

Abstract

Polyacrylamide gels with different stiffness and glass were employed as substrates to investigate how substrate stiffness affects the cellular stiffness of adherent hepatocellular carcinoma (HCCLM3) and hepatic (L02) cells. The interaction of how cell–substrate stiffness influences cell migration was also explored. An atom force microscope measured the stiffness of HCCLM3 and L02 cells on different substrates. Further, F-actin assembly was analyzed using immunofluorescence and Western blot. Finally, cell-surface expression of integrin $\beta 1$ was quantified by flow cytometry. The results show that, while both HCCLM3 and L02 cells adjusted their cell stiffness to comply with the stiffness of the substrate they were adhered to, their tuning capabilities were different. HCCLM3 cell stiffness complied when substrate stiffness was between 1.1 and 33.7 kPa, whereas the analogous stiffness for L02 cells occurred at a higher substrate stiffness, 3.6 kPa up to glass. These ranges correlated with F-actin filament assembly and integrin $\beta 1$ expression. In a migration assay, HCCLM3 cells migrated faster on a relatively soft substrate, while L02 cells migrated faster on substrates that were relatively rigid. These findings indicate that different tuning capabilities of HCCLM3 and L02 cells may influence cell migration velocity on substrates with different stiffness by regulating cytoskeleton remodeling and integrin $\beta 1$ expression.

© Koninklijke Brill NV, Leiden, 2012

Keywords

Relative cell–substrate stiffness, cytoskeleton assembly, integrin $\beta 1$ expression, cell migration, adaptation range, hepatic carcinoma cells

* To whom correspondence should be addressed. E-mail: cquliyang@hotmail.com

1. Introduction

In vitro studies have shown that cellular functions, such as spreading [1], migration [2], proliferation [3, 4], differentiation [5, 6] and apoptosis [4, 7], of adherent cells are correlated with the stiffness of the substrate to which they attach. For example, fibroblasts and endothelial cells prefer to spread on stiffer substrates [1], whereas neurons branch more avidly on softer surfaces [8]. Similarly, on gels softer than 200 Pa (shear modulus), neurons proliferate, but astrocytes do not survive [9]. Stem cell differentiation into distinct lineages also depends on the substrate's stiffness [10, 11]. For instance, neural stem cells adhered to softer gels (100–500 Pa, Young's modulus) differentiate into neurons, while adhesion to stiffer gels (1000–10 000 Pa) promotes differentiation into glial cells.

Solon *et al.* [12] proposed that the interaction of cell stiffness and substrate stiffness may contribute to changes in cell behaviors and cell-type-dependent responses on various substrates. They found that fibroblasts cultured on flexible substrates with various stiffness values were only able to tune their cell stiffness to comply with that of the substrates they adhered to, thereby regulating their cell spreading in a particular range of substrate stiffness. In a study on how substrate rigidity affects cell morphology and migration, a mathematical model demonstrated that the relative rigidity between a cell and its substrate is more essential than the substrate rigidity itself [13]. The model is based on the competition between elastic energies in the cell–substrate system and interfacial energies of adhesion at the cell periphery. Recent studies have shown that metastatic tumor cells from lung, breast and pancreatic cancers are softer than their normal counterparts [13, 14]. However, how cell stiffness changes that effect on the relative rigidity between the cell and its substrate can alter the cell's response, including changes in integrin expression and cytoskeleton assembly, and impacts cell migration behavior, is still unknown. This study investigates the effect of the relative cell–substrate rigidity on cell migration by analyzing the response of hepatic (L02) and hepatocellular carcinoma (HCCLM3, abbreviated M3) cells adhered to substrates that vary in stiffness.

We measured the stiffness of cells adhered to either polyacrylamide (PA) substrates that varied in stiffness or glass, and observed that L02 cells and M3 cells altered their modulus to comply with substrate stiffness at different ranges of substrate stiffness. The range of substrate stiffness that promotes actin cytoskeleton assembly and regulates integrin β 1 expression was also studied in adherent L02 and M3 cells and found to correlate with the cell-substrate modulus compliance range. Finally, we found that M3 cells migrated faster than L02 cells on a substrate rigidity that is close to liver tissues, indicating that the metastatic potential of hepatic carcinoma cells may be provoked before liver tissue becomes cirrhotic.

2. Materials and Methods

2.1. Fabrication and Mechanical Characterization of the Gels

The stiffness of PA gels was regulated by adjusting the ratio of acrylamide (Sigma) to bis-acrylamide (Sigma) as described previously [15]. Briefly, PA gel solutions

were prepared using acrylamide solutions at final concentrations of 5.5, 7.5 and 12% (w/v) and bis-acrylamide concentrations from 0.06 to 0.3% (w/v). Human plasma fibronectin (Fn, Sigma) was cross-linked onto PA gel surfaces with a heterobifunctional cross-linker, sulfo-SANPAH (sulfosuccinimidyl 6-(4'-azido-2'-nitrophenylamino hexanoate), Pierce 22589). First, the top surface of the gel was completely covered with a 1 mM sulfo-SANPAH solution and then irradiated for 10 min using an ultraviolet lamp. This entire process (coating–irradiation) was then repeated. Excess cross-linker was removed through three 3-ml washes with 200 mM HEPES (pH 8.6). Next, 200 μ l Fn solution (2.5 μ g/ml in HEPES) was added to the PA gel and allowed to react for 12 h at 4°C. Fn-coated PA gels were washed twice with RPMI-1640 medium to remove any unbound Fn prior to cell seeding.

The viscoelastic properties of PA gels were quantified using a rheometer (TA Instruments, AR2000ex). The shear modulus (G') was determined from the shear stress in phase with the oscillatory frequency of 0.2 Hz and maximum shear strain (amplitude) of 1%, at 37°C. From the shear modulus (G'), the elastic modulus (E) of the PA gel was calculated, assuming that all of the PA gels tested are incompressible and have a Poisson's ratio of 0.5; i.e., $E = 3 \times G'$.

The Young's moduli values for each of the substrates utilized in this study are as follows: 1.1 ± 0.2 kPa for 5.5% acrylamide, 0.06% bisacrylamide; 3.6 ± 0.6 kPa for 5.5% acrylamide, 0.1% bisacrylamide; 10.7 ± 1.2 kPa for 7.5% acrylamide, 0.2% bisacrylamide; and 33.7 ± 1.1 kPa for 12% acrylamide, 0.3% bisacrylamide.

2.2. Cell Culture

The human hepatocellular carcinoma cell line HCCLM3 (abbreviated M3) is a highly metastatic pulmonary cell line that was established from the human HCC lung metastases of nude mice. The human hepatic cell line (L02) is derived from primary human liver cells that were immortalized by the Simian Virus 40 large T antigen gene and acts as the normal control for M3 cells. Both M3 and L02 cell lines were obtained from the Fudan University Zhong Shan Hospital Liver Cancer Research Institute. M3 and L02 cells were cultured in RPMI-1640 medium supplemented with 10% fetal calf serum (FCS) at 37°C and 5% CO₂. Experiments were conducted prior to 20 cell passages.

2.3. Atomic Force Microscopy

Cell stiffness was quantified by atomic force microscopy (AFM) (JPK Instruments, NanoWizard II). Mechanical measurements were obtained at room temperature using quadratic pyramid cantilevers with a nominal stiffness of 0.04 N/m. The half-angle to face of the AFM tip was 17.5°, and the Poisson ratio of the cell was taken to be 0.5, which is typical for soft biological materials. Using AFM software, the tip was precisely positioned over the perinuclear region, between the spreading edge and the nucleus. All measurements were obtained in tapping mode. Force–displacement curves were recorded on each cell to determine their apparent cell stiffness and then converted into force–indentation curves in order to calculate Young's modulus, or E .

2.4. Immunofluorescence

For immunofluorescence, cells were fixed with 4% paraformaldehyde, washed with PBS twice, and then permeabilized with 0.5% Triton X-100. Cells were stained with 0.5 µg/ml Rhodamine-phalloidin (Sigma) to detect the actin cytoskeleton and 0.1 µg/ml 4',6-diamidino-2-phenylindole (DAPI, Sigma) to detect the nucleus. After washing with PBS, fixed cells were visualized on a Leica microscope under a 100× oil immersion objective lens.

2.5. Western Blot

Cross-linked F-actin on cells that had adhered to glass or PA gels that varied in stiffness was assayed by Western blot. After 24 h of culturing, L02 and M3 cells were washed with ice-cold PBS and harvested with a scraper into chilled RIPA buffer (50 mM Tris (pH 7.5), 150 mM NaCl, 1% NP-40, 0.25% sodium pyrophosphate, sodium orthovanadate, EDTA, sodium fluoride, leupeptin). The cell suspension was then ultrasonicated on ice 20 times for 4 s at intervals of 10 s. The protein concentrations of each sample were measured using a bicinchoninic acid (BCA) protein assay kit (Biotek). Equal amounts of total protein from each sample were centrifuged at 12 000 rpm for 20 min at 4°C. The supernatant was discarded and the insoluble pellet containing all of the cross-linked actin filaments in the cell was resuspended and lysed with 1% SDS buffer (50 mM Tris (pH 8.1), sodium pyrophosphate, β-glycerophosphate, sodium orthovanadate, sodium fluoride, EDTA, leupeptin). Cell lysates were separated by SDS-PAGE and transferred to a polyvinylidene difluoride (PVDF) membrane. After transfer, the PVDF membrane was blocked using 5% bovine serum albumin (Sigma) and incubated with a rabbit anti-human β-actin (1:2000; CST) primary antibody overnight. The membrane was then washed with 0.2% Tween in Tris-buffered saline (TBST) and incubated with peroxidase conjugated goat anti-rabbit IgG (1:1000; CST) for 1 h. Antibodies were detected by enhanced chemiluminescence (ECL). Bands were scanned by a densitometer (Bio-Rad) and quantified with Quantity One 4.6.3 software (Bio-Rad).

2.6. Flow Cytometry

A total of 1×10^6 cells was allowed to adhere on either PA gels that varied in stiffness or on glass. After 24 h, adherent cells were detached from the substrates using a Trypsin-EDTA solution and washed with PBS. Cells were then resuspended in PBS containing FITC-conjugated mouse anti-human integrin β1 (Abbiotec) antibody for 1 h on ice. Cells incubated with FITC-conjugated mouse IgG isotype in the absence of primary antibody served as negative controls. The integrin β1 expression was measured by flow cytometry (BD FACSCalibur). The relative cellular fluorescence intensity ratio was calculated as the sample's fluorescence intensity over the fluorescence intensity of the negative controls.

2.7. Cell Migration

Cell migration on the PA gels as well as on glass surfaces coated with 2.5 µg/ml Fn was monitored by time-lapse microscopy. Because cell–cell contacts affect cell

migration, only those cells without contact to adjacent cells were analyzed. Single-cell speed was represented by the total length of the path divided by time. The centroid of the cell was tracked in 5 min intervals over a period of 1 h by time-lapse image sequences using Image J software (<http://rsbweb.nih.gov/ij/>).

2.8. Statistical Analysis

The data are presented as the mean \pm SD from at least three independent experiments. Statistical analysis was performed using Sigma plot and Student's *t*-test analysis. A *P* value < 0.05 was considered statistically significant.

3. Results

3.1. Effects of Substrate Stiffness on the Stiffness of L02 and M3 Cells

Figure 1 gives the AFM measurement of Young's modulus (*E*) for L02 and M3 cells adhered to substrates with varying stiffness. Overall, the moduli of L02 and M3 cells increased with substrate stiffness. However, the stiffness range that a cell complied with was different between the two cell lines. The modulus for L02 cells started to increase when the substrate with Young's modulus was near 3.6 kPa and continued to increase up until high rigidity (glass). In contrast, the increase for M3 cells started near 1.1 kPa and reached an asymptote at a substrate stiffness of 33.7 kPa.

3.2. Actin Cytoskeleton Assembly and Integrin $\beta 1$ Expression on Substrates with Different Stiffness Values

Rhodamine-labeled phalloidin was used to stain actin in L02 and M3 cells. As shown in Fig. 2a, the actin in L02 cells that had adhered to a 1.1 kPa substrate localized in a ring along the cell periphery, assembled into a network on substrates

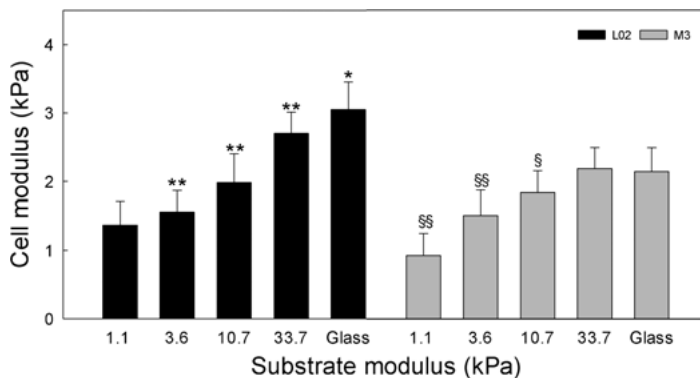


Figure 1. Young's modulus of L02 and M3 cells on substrates with different stiffness measured by AFM. The data are given as the mean \pm SD from four separate experiments ($n \geq 15$ for each condition). * and § indicate that the value of the column is significantly lower than the next adjacent column for L02 and M3 cells, respectively (**, §§ $P < 0.01$, *, § $P < 0.05$).

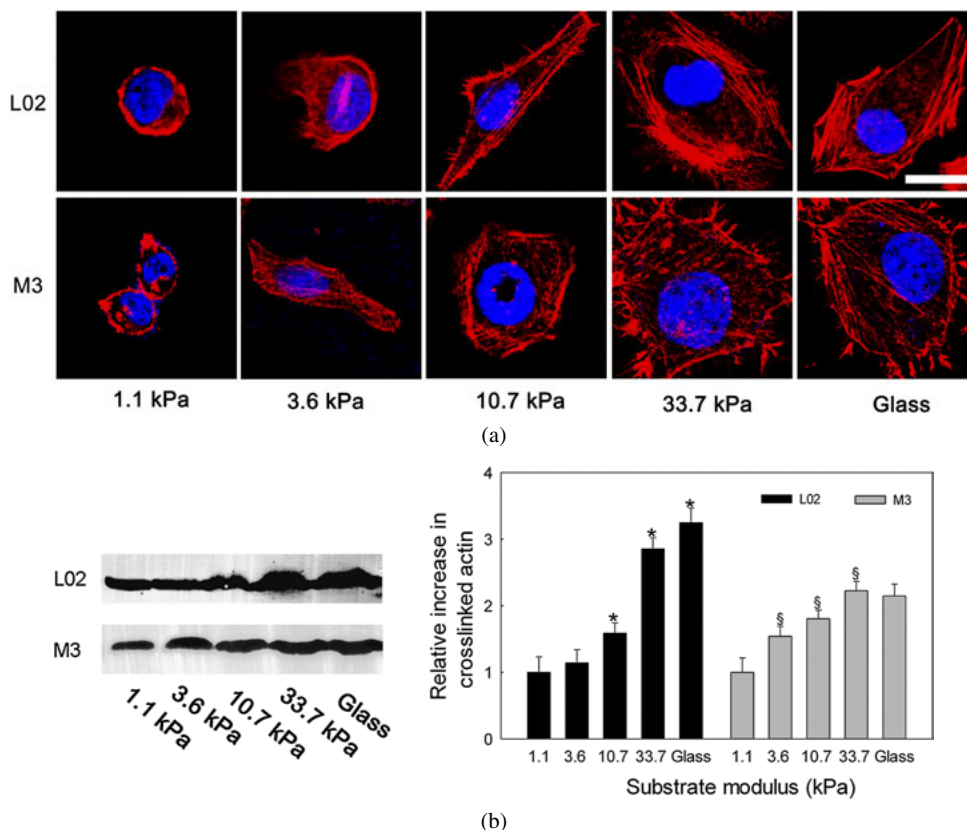


Figure 2. Observation and quantification of F-actin assembly on different substrates by immunofluorescence and Western blot of L02 and M3 cells. (a) Immunofluorescence assay. F-actin is in red and nuclei are in blue. Scale bar = 15 μm . (b) Western blot assay to detect cross-linked F-actin filaments on different substrates. Bands were quantified by Quantity One software. One representative experiment out of three is shown. *,§ $P < 0.05$, significantly lower column value than the next adjacent column for L02 and M3 cells, respectively. This figure is published in colour in the online edition of this journal, which can be accessed via <http://www.brill.nl/jbs>

of 10.7–33.7 kPa, and showed an increase in cross-linking of filaments on glass. Actin assembly in M3 cells also exhibited a similar dependency on substrate stiffness as L02 cells. However, unlike L02 cells, the cross-linked F-actin filaments of M3 cells were tenuous, and no pronounced actin filament bundles were observed in M3 cells adhered to glass.

As shown in Figs 2b and 3, both L02 and M3 cells exhibited an increase in actin filament cross-linking and integrin $\beta 1$ expression on the various substrates utilized in this study. The increased tendency for actin to cross-link and the higher integrin $\beta 1$ expression correlate well with the cell's modulus. For L02 cells adhered to substrates with stiffness values from 3.6 kPa to high rigidity (glass), the cross-linking of actin filaments and integrin $\beta 1$ expression increased as the substrate became stiffer,

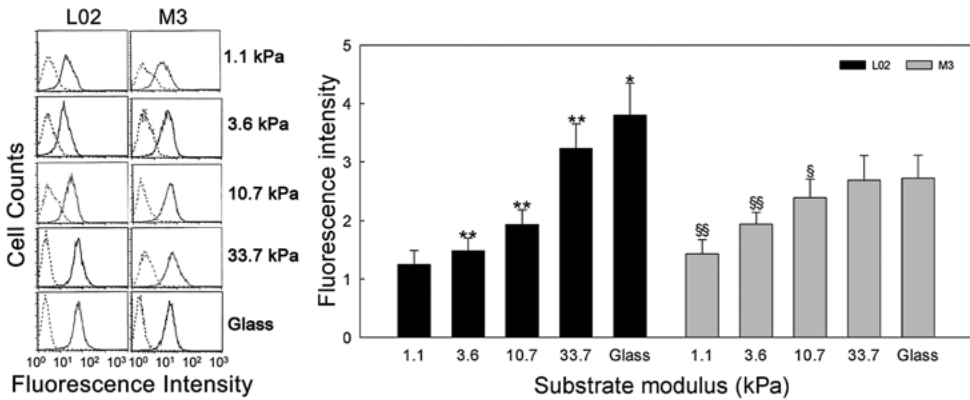


Figure 3. Cellular integrin $\beta 1$ expression in L02 and M3 cells on different substrates, determined by flow cytometry. Solid lines indicate the sample fluorescence intensity, and the dotted lines indicate the negative control fluorescence intensity. The data are given as the mean \pm SD from three separate experiments. **, §§ $P < 0.01$, *, § $P < 0.05$, significantly lower column value than the next adjacent column for L02 and M3 cells, respectively.

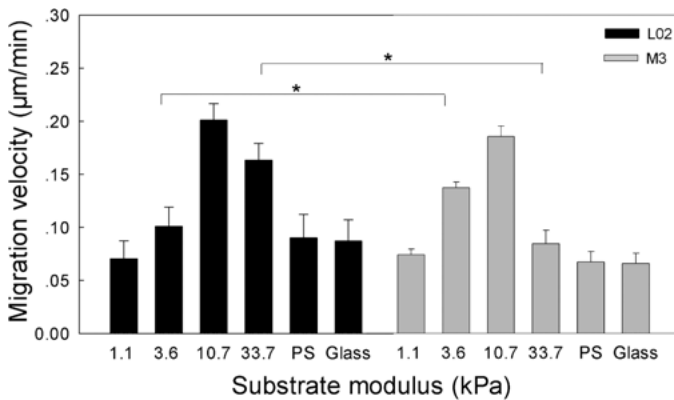


Figure 4. Cell migration velocity on substrates with different stiffness. The results are mean \pm SD from three separate experiments ($n \geq 10$ for all conditions). * $P < 0.05$, significantly different migration velocity between L02 and M3 cells adhered to 3.6 and 33.7 kPa gels.

while M3 cells exhibited these features when adhered to substrates with stiffnesses of 1.1–33.7 kPa.

3.3. Cell Migration on Substrates with Different Stiffness

The result from Fig. 4 shows that cell migration velocity is strongly influenced by substrate stiffness. L02 and M3 cells exhibit similar general trends for cell migration velocity on substrates that vary in stiffness. For both cell types, migration velocity increased with substrate stiffness, peaked at the substrate modulus of 10.7 kPa, and then decreased as substrates became more rigid. However, on a substrate of 3.6 kPa, L02 cells displayed a lower migration velocity than M3 cells, whereas on a substrate of 33.7 kPa, L02 cells showed a higher migration velocity than M3 cells.

4. Discussion

Tractions are generated by cytoskeleton organization in an adherent cell and transmitted into the substrate through integrin linkages [16, 17]. Cellular traction has been reported to increase with substrate rigidity and has a maximum limit that depends on the cell's properties [18]. The increase in cellular traction reflects a cell's increased stiffness in response to substrate rigidity. The result in Fig. 1 demonstrates that a 'stiffening' phenomenon (or tuning capability) was observed in both L02 and M3 cells. A mathematical model [12] can explain cell stiffening, which is associated with cytoskeleton assembly, on flexible substrates. When cells adhere to a substrate, cellular traction is formed at cell–substrate adhesion sites. As a result, the substrate deforms. Based on the force balance between the cell and its substrate, the model is depicted as follows:

$$E_c(\varepsilon_c)\varepsilon_c = E_s\varepsilon_s, \quad (1)$$

where E_c and E_s are the elastic moduli, while ε_c and ε_s are the cell strains and substrate, respectively. Based on a previous study [19], E_c is a function of ε_c , according to the strain stiffening of cells, and E_s represents a linear gel of constant stiffness. As long as $E_c < E_s$, the deformation of a cell caused by the cytoskeleton will be greater than the deformation caused by the substrate. As a cell continues to deform, cytoskeletal actin assembly continues. Thus, the stiffness of a cell will increase with ε_c and reach a limit so that equation (1) is balanced. Based on this reasoning, and as the results in Fig. 1 show, the modulus of L02 cells can be stiffened from 1.4 to 3 kPa when they adhere to substrates that range from 3.6 kPa to high rigidity (glass). The modulus of M3 cells increases from 0.9 to approx. 2 kPa, but once they adhere to a substrate, the modulus ranges from 1.1 to 33.7 kPa. These results indicate that L02 cells have a different adaptation range compared to M3 cells. In this adaptation range of substrate stiffness, cells interact with the substrate and are able to respond to the substrate with different rigidity.

Similar to the results found here, previous studies have found that cytoskeleton constituents and accessory proteins decrease during the transformation of a normal cell to a cancerous cell [20, 21]. As shown in Fig. 2, M3 cells had fewer and thinner cytoskeletal fibers compared to L02 cells. The differences in cytoskeletal organization between L02 and M3 cells adhered to substrates may be the result of differences in the cell modulus, subsequent to the dissimilarity in the rigidity adaptation range between L02 and M3 cells.

The magnitude of AFM indentation is relatively small (<400 nm) in a cell compared to the height of the cell (approx. 8 μm). Therefore, the cell modulus shown in Fig. 1 reflects the cortical stiffness rather than the overall stiffness of the cell [12], which is difficult to detect due to technical limitations. However, in a separate study on the association between cell morphology and substrate stiffness, we found that the sensitive interaction range of M3 cells is different from L02 cells (data not shown). This confirms the range we found in this study. Within the sensitive

interaction range, cells were able to tune their stiffness and comply with the substrate stiffness through assembly of the actin cytoskeleton. The extent of assembly not only contributes to the cell modulus [22], but also influenced the expression of integrin $\beta 1$ [16].

Integrins link cytoskeleton to substrate at adhesion complexes. Thus, integrins transmit both the external force to, as well as the internal traction force from, the cytoskeleton through adhesion sites. This traction also promotes the expression of integrins on the cell surface [17]. As a result, cell and substrate stiffness, cytoskeleton assembly, and integrin $\beta 1$ expression form an integrated circuit that collectively influences the velocity of cells migrating on substrates with different rigidity. On soft gels, unassembled actin could not generate enough traction force to increase integrin $\beta 1$ expression, implying a poor adhesion contact between the cell and its substrate. These findings indicate that soft gels are not favorable to cell migration (low velocity). Conversely, on rigid surfaces, high resistance from the substrate enhances cross-linking of actin filaments, which then increases integrin $\beta 1$ expression in these cells. This type of organization hampers cytoskeleton remodeling and the turnover of focal adhesions, which are essential for cell migration. As a result, the migration velocity on a rigid substrate is slower. On surfaces exhibiting moderate stiffness, the force between the cell and its substrate are thought to achieve a high migration velocity. Our results shown in Fig. 4 are consistent with this notion. We found that, compared to a 1.1 kPa substrate, the integrin $\beta 1$ expression and cytoskeleton assembly of M3 cells increased on a 3.6 kPa substrate, while no increase was observed in L02 cells. The increased integrin $\beta 1$ expression and cytoskeleton assembly could account for the higher migration velocity of M3 cells adhered to a 3.6 kPa substrate.

The data presented here show that L02 and M3 cells have different abilities in altering their stiffness to adapt to substrate rigidity. Regulating cytoskeleton organization and integrin $\beta 1$ expression may also contribute to the difference in cell migration velocity on substrates that vary in stiffness. The different adaptation ranges of substrate rigidity between L02 and M3 cells may contribute to the initiation of hepatic carcinoma cell metastasis. According to our observations of cell migration velocity, M3 cells exhibited a higher migration potential than L02 cells on a 3.6 kPa substrate. This tumor cell potential could weaken tumor cell–cell adhesion, perturb tissue architecture, and facilitate tumor cell detachment from primary tissue [23, 24]. Previous studies suggest that metastatic progression of tumor cells depends on tissue rigidity [25, 26]. A 3.6 kPa substrate is close to the rigidity of normal liver tissue (approx. 4 kPa) [27]. These findings indicate that the metastatic potential of liver cancer cells may be activated in an environment found in liver tissues where normal liver cells maintain quiescence. Although the results presented in this study are from a single pair of cell lines, our results pave the path for investigating other cell lines and will help solidify conclusions on how cell activity correlates to substrate stiffness.

Acknowledgements

This work was supported in part by grants from the National Nature Science Foundation of China (Nos 11032012, 30870608 and 10472137), the Innovation and Attracting Talents Program for College and University ('111' Project) (B06023), the Key Science and Technology Program of CQ CSTC (CSTC, 2009AA5045) and the sharing fund of Chongqing University's large-scale equipment.

References

1. T. Yeung, P. C. Georges, L. A. Flanagan, B. Marg, M. Ortiz, M. Funaki, N. Zahir, W. Ming, V. Weaver and P. A. Janmey, *Cell Motil. Cytoskeleton* **60**, 24 (2005).
2. K. M. Stroka and H. Aranda-Espinoza, *Cell Motil. Cytoskeleton* **66**, 328 (2009).
3. N. D. Leipzig and M. S. Shoichet, *Biomaterials* **30**, 6867 (2009).
4. H. B. Wang, M. Dembo and Y. L. Wang, *Am. J. Physiol. Cell Physiol.* **279**, C1345 (2000).
5. N. D. Evans, C. Minelli, E. Gentleman, V. LaPointe, S. N. Patankar, M. Kallivretaki, X. Chen, C. J. Roberts and M. M. Stevens, *Eur. Cell Mater.* **18**, 1 (2009).
6. B. van der Sanden, M. Dhobb, F. Berger and D. Wion, *J. Cell Biochem.* **111**, 801 (2010).
7. Y. H. Zhang, C. Q. Zhao, L. S. Jiang and L. Y. Dai, *Matrix Biol.* **30**, 135 (2011).
8. L. A. Flanagan, Y. E. Ju, B. Marg, M. Osterfield and P. A. Janmey, *Neuroreport* **13**, 2411 (2002).
9. P. C. Georges, W. J. Miller, D. F. Meaney, E. S. Sawyer and P. A. Janmey, *Biophys. J.* **90**, 3012 (2006).
10. K. Saha, A. J. Keung, E. F. Irwin, Y. Li, L. Little, D. V. Schaffer and K. E. Healy, *Biophys. J.* **95**, 4426 (2008).
11. A. J. Engler, S. Sen, H. L. Sweeney and D. E. Discher, *Cell* **126**, 677 (2006).
12. J. Solon, I. Levental, K. Sengupta, P. C. Georges and P. A. Janmey, *Biophys. J.* **93**, 4453 (2007).
13. S. E. Cross, Y. S. Jin, J. Rao and J. K. Gimzewski, *Nature Nanotechnol.* **2**, 780 (2007).
14. T. W. Remmerbach, J. Kas, J. Runge and J. Guck, *Oral Dis.* **16**, 519 (2010).
15. K. A. Beningo, C. M. Lo and Y. L. Wang, *Methods Cell Biol.* **69**, 325 (2002).
16. M. B. Asparuhova, L. Gelman and M. Chiquet, *Scand. J. Med. Sci. Sports* **19**, 490 (2009).
17. A. Katsumi, A. W. Orr, E. Tzima and M. A. Schwartz, *J. Biol. Chem.* **279**, 12001 (2004).
18. J. P. Califano and C. A. Reinhart-King, *Cell. Mol. Bioeng.* **3**, 68 (2010).
19. P. Fernandez, P. A. Pullarkat and A. Ott, *Biophys. J.* **90**, 3796 (2006).
20. J. Guck, S. Schinkinger, B. Lincoln, F. Wottawah, S. Ebert, M. Romeyke, D. Lenz, H. M. Erickson, R. Ananthkrishnan, D. Mitchell, J. Kas, S. Ulvick and C. Bilby, *Biophys. J.* **88**, 3689 (2005).
21. E. Friedman, M. Verderame, S. Winawer and R. Pollack, *Cancer Res.* **44**, 3040 (1984).
22. K. Bhadriraju and L. K. Hansen, *Exp. Cell Res.* **278**, 92 (2002).
23. R. J. Burkhalter, J. Symowicz, L. G. Hudson, C. J. Gottardi and M. S. Stack, *J. Biol. Chem.* **286**, 23467 (2011).
24. M. J. Paszek, N. Zahir, K. R. Johnson, J. N. Lakins, G. I. Rozenberg, A. Gefen, C. A. Reinhart-King, S. S. Margulies, M. Dembo, D. Boettiger, D. A. Hammer and V. M. Weaver, *Cancer Cell* **8**, 241 (2005).
25. M. J. Paszek and V. M. Weaver, *J. Mammary Gland Biol. Neoplasia* **9**, 325 (2004).
26. J. T. Erler and V. M. Weaver, *Clin. Exp. Metastasis* **26**, 35 (2009).
27. M. Yoneda, H. Mawatari, K. Fujita, H. Endo, H. Iida, Y. Nozaki, K. Yonemitsu, T. Higurashi, H. Takahashi, N. Kobayashi, H. Kirikoshi, Y. Abe, M. Inamori, K. Kubota, S. Saito, M. Tamano, H. Hiraishi, S. Maeyama, N. Yamaguchi, S. Togo and A. Nakajima, *Dig. Liver Dis.* **40**, 371 (2008).